

Formulation of Snow Depth Algorithms for Different regions of NW-Himalaya using Passive Microwave Satellite Data

Dhiraj Kumar Singh^{1,*}, K.K.Singh², V.D.Mishra² and J.K.Sharma¹

1. Rayat Institute of Engineering & Information Technology, S.B.S Nagar, Punjab 144533 India.

2. Snow and Avalanche Study Establishment, Defense Research and Development Organization, Chandigarh 160036 India.

Abstract

Seasonal snows cover in NW-Himalaya plays an important role in hydrological and avalanche studies and also act as an indicator of climate change. However, due to ruggedness and inaccessibility of Himalayan terrain, it is very difficult to monitor the snow cover using conventional measurement techniques. Remote sensing based satellite data provide solution to monitor seasonal snow cover variations and to study snow cover characteristic.

In this study brightness temperature (T_B) of snow has been estimated using special sensor microwave imager (SSM/I) satellite data and the spectral and temporal variation of T_B were studied. These T_B values in combination with scattering index (SI) were used to detect the presence or absence of snow covered areas. The threshold values of T_B and SI were estimated for snow cover area of different Himalayan ranges. Algorithms for snow depth estimation were developed using T_B and ground observatories data from different ranges of the NW-Himalaya. The developed algorithms were validated using one year satellite data. A good correlation was observed between the predicted and manually observed snow depth values i.e. 0.84 for Karakoram, 0.77 for Great Himalayan range and 0.60 for Pir-Panjol.

Key words: SSM/I, Scattering Index, Snow depth and Brightness temperature.

1. Introduction

Snow cover has the largest area extent of any component of cryosphere, with most of snow covered area located in Northern Hemisphere.

Remote sensing based techniques are useful tool for gathering information of vast area and also capable of deducing land, ocean and atmospheric parameter [1]. These are also used successfully for study of snow properties and global water cycle [2, 3]. Various researcher have used optical and microwave satellite data for snow cover monitoring. The Optical data is useful for estimation of snow surface properties and also for estimation of areal extent of snow. However, one of the major problem with the use of optical data in winter is cloud cover, as in NW Himalaya in winter most of area remains under clouds and because of lower wavelength of optical satellite data, it will not be able to penetrate the clouds. Thus, during cloudy days the use of optical data will not provide the snow cover information. However, microwave satellite data can be used to provide snow cover information in all weather condition because of its high penetration power. Microwave satellite data can be used for estimation of volume properties of snow i.e. snow depth and snow water equivalent (SWE) etc. Microwaves are sensitive to snow parameter such as grain size and wetness of snow [4]. Passive microwave remote sensing data can be used for retrieval of useful parameters, such as emissivity and snow depth etc. But the resolution is the disadvantage of the passive microwave data, which is very coarse compared to available optical satellite data.

SSM/I measure the brightness temperature (T_B) of land cover. The T_B is highly dependent on frequency and polarizations. The T_B of snow decreases with increase of frequency. As T_B is the product of snow pack/snow surface temperature (T_S) and emissivity (ϵ), it shows significant variation from month to month and this variation is due to variation in snow pack/snow surface temperature. Snow is highly scattering material. The scattering from the snow particle attenuate the radiation as it passes from snow cover. This attenuation

generally increases with the increase of frequency of wave, grain size and increase of snow depth [5].

Most of research related to snow depth estimation was carried out at relatively homogeneous flat area such as the Canadian high plains and Russian steppes. Passive microwave data was used to derive snow depth from flat homogeneous area [4]. SSM/I data was used to estimate snow depth from one of the location of Indian Himalaya [6]. However, the developed equation directly can not be used to estimate snow depth from any other location of Great Himalaya.

vertical polarization. The incident angle at surface is 53.3° , the effective field of over view ranges from 69 km x 43 km (19 GHz) to 15 km x 13 km (85 GHz). In this study SSM/I data of the period 2007 to 2011 has been analyzed to retrieve the threshold values of T_B and SI and six years of data (2007-2011 and 2001-2003) has been used to formulate the snow depth algorithms. The snow meteorological data was used from different field observatories of SASE situated at different Himalayan ranges.

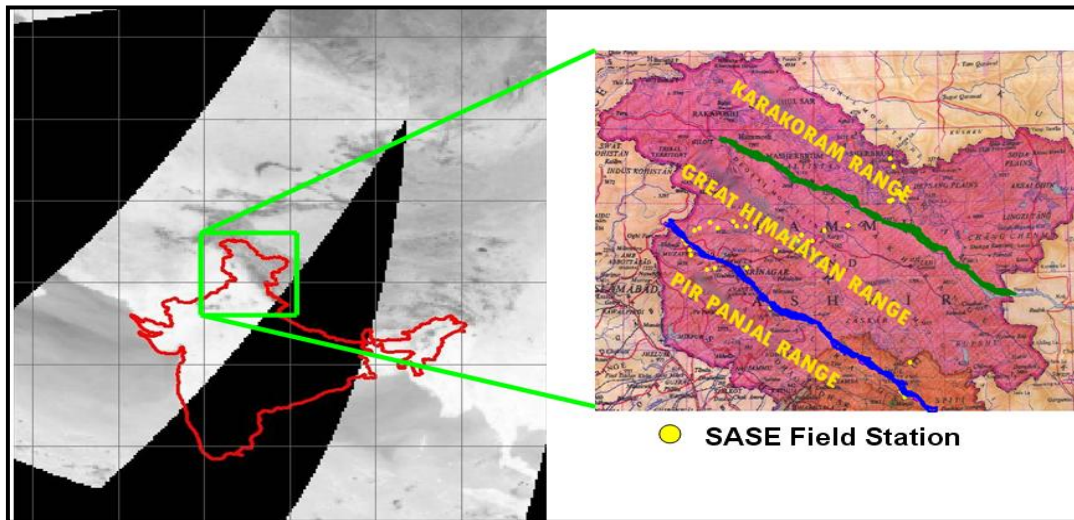


Figure 1. Study area of NW Himalaya with different ranges and SASE field locations.

In this study passive microwave SSM/I satellite data is used to estimate the T_B values at different frequencies. The T_B maps were made and the temporal and spectral variations of T_B values were studied. The scattering index (SI) is estimated and the combination of T_B and SI is further used to discriminate between snow and non-snow area. For that the threshold values of T_B and SI for different Himalayan ranges have been estimated. Snow depth algorithms were developed using T_B and respective ground observatories data for different Himalayan ranges.

2. Data Used

The special sensor microwave imager (SSM/I) satellite data is used in the present study. SSM/I is near polar sensor at an altitude of 833 km with an inclination of 98.8° and an orbit period of 102 minutes. With a swath width of almost 1400 km, SSM/I provides near global coverage every day. SSM/I scans the earth surface at frequencies 19.3, 37 and 85.5 or 91 GHz in vertical and horizontal polarization and at 22.2 GHz in

3. Study Area

Present study is concentrated in Indian Himalayan region shown in Figure 1, which stretches from east to west for about 2500 Km across 72°E to 80°E longitude and 29°N to 37°N latitude.

NW Himalaya has been categorized into different ranges i.e. lower Himalaya (Pir-Panjal range), middle Himalaya (Great Himalayan range) and upper Himalaya (Karakoram range) [8]. Pir-Panjal range experiences heavy snowfall between Decembers to March. The average altitude of Pir-Panjal range lies between 2000 to 4000m. The temperature of this range generally remains high in comparison to other two Himalayan ranges. Great Himalayan range has relatively less temperatures and snowfall than Pir-Panjal range. It receives dry snow between mid December and end of January. The general rise in temperature from mid February onwards moistens fresh snowfall and after March the fresh snowfall is often accompanied with wet snowfall or light rain. Altitude of this range varies from 3500 to 5300 m. Very low temperatures have been observed in Karakoram range

and thus snow remains dry in most of the time. Its altitude is more than 5000m [7]. Thus overall NW Himalaya is having different snow characteristic in different area, which affects local weather and energy balance of the region and also play role in avalanche initiation [8].

4. Methodology

The SSM/I satellite data was copied directly from NSIDC website and ENVI and ArcGIS software's were used for processing of the data.

Temporal and spectral variations of brightness temperature values were drawn. As snow is highly scattering material, thus the SI values were calculated using different frequencies of SSM/I. T_B at different frequencies (i.e. 19, 37 and 85 GHz for horizontal polarization) and SI were estimated and further compared with ground observed snow meteorological data. Further the threshold values of T_B at different frequencies and SI were estimated for different ranges of NW Himalaya and used for discrimination between snow and non snow areas.

T_B values corresponding to the different frequencies were estimated for different ground observatory location (SASE) in NW-Himalaya. These estimated T_B values were further used to estimate the SI.

$$SI = \text{Max} (T_{B22V} - T_{B85V}, T_{B19V} - T_{B37V}) \quad (1)$$

Where SI is scattering index and T_{B19} , T_{B22V} , T_{B37V} , T_{B85V} are the T_B at 19, 22, 37 and 85 GHz frequencies at vertical polarization.

T_B values are affected by the amount of snow present at the ground. In order to formulate the snow depth algorithm regression analysis was performed between T_B and ground observed snow depth values. To develop the snow depth algorithms for different ranges of NW Himalaya 6 year passive microwave satellite data was used along with the ground data from various SASE observatories. T_B values of 19 GHz (H), 37 GHz (H) and 85 GHz (H) channels were used in these algorithms.

In order to develop the algorithms, NW Himalaya was divided into three ranges i.e. lower, middle and upper Himalaya. In the algorithm development part we have taken ground data from all observatories falling in the respective ranges and different combination of frequencies were used to formulate the snow depth equation. In this study, we have included data of thirteen ground observatories from Pir-Panjaj, nine ground observatories each from Great Himalayan and Karakoram range respectively. The equations for snow depth estimation were given below.

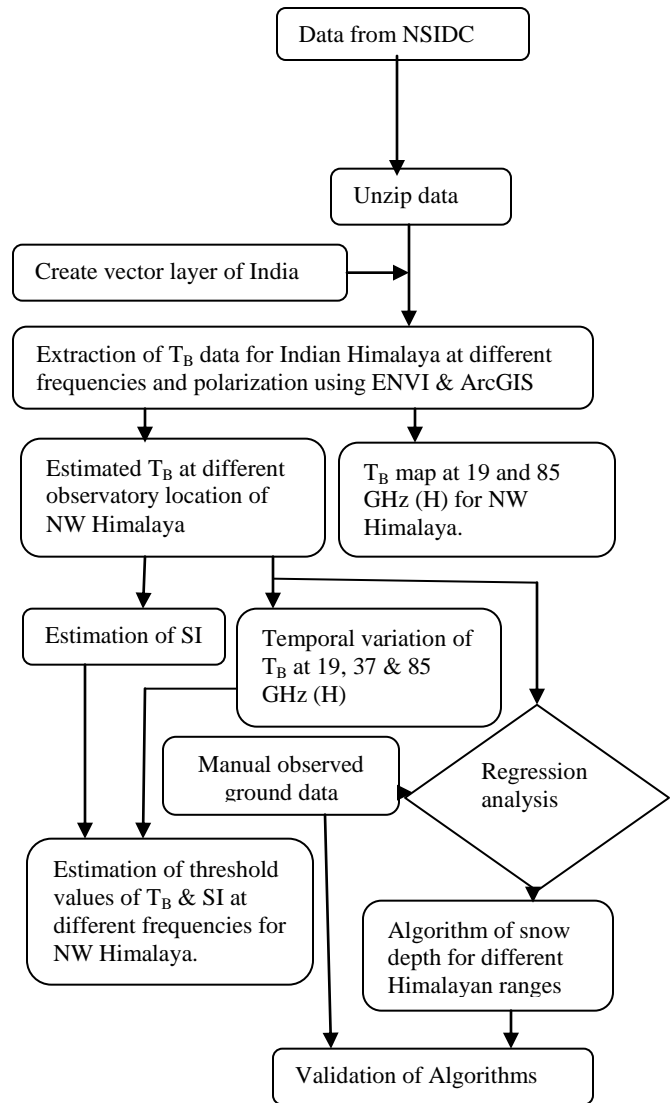


Figure 2: Flow chart of methodology

$$SD = a1*(T_{B85H}) + b1 \quad \text{for 5 cm (2)}$$

$$SD = a2*(T_{B37H}) + b2 \quad \text{for 50 cm (3)}$$

$$SD = a3*(T_{B19H} - T_{B37H}) + b3 \quad \text{for 200 cm (4)}$$

Where T_{B85H} , T_{B37H} and T_{B19H} are T_B at 85, 37 and 19 GHz at horizontal polarization.

The constant in the above mentioned equation were estimated using the least square cure fit method. Further these equations were applied on 1 year satellite data for the validation of the developed equations. The correlation and the root mean square error (RMSE) between the grounds observed snow depth values and satellite data estimated snow depth values were further estimated.

5. Results and Discussion

The T_B is highly dependent on frequency and polarizations. As T_B is the product of snow pack/snow surface temperature (T_S) and emissivity (ϵ), the T_B shows significant variation from month to month and this variation is due to variation in snow pack/snow surface temperature in respective months.

Figure.3 shows the spatial and temporal variation of T_B at 19GHz (H) frequency for NW Himalayan ranges from year 2007 to 2008. From figure, it is observed that Pir-Panjaj range is showing higher T_B values in comparison to other two ranges. The T_B of snow pack depends on various snow pack properties and on the ambient/snow pack temperature. In Pir-Panjaj range the ambient temperature generally remains higher in comparison to other ranges, thus its T_B is also observed higher. While in Karakoram range due to very low ambient temperature low T_B values were observed. However, the range of T_B values in Greater Himalaya is observed in mid of Karakoram and Pir-Panjaj ranges.

From figure.4, it is observed that from April onwards the T_B values are much higher which shows the start of melting of the snow as during melting the water coats the snow grain or due to more moisture in the snow the snow behavior starts shifting towards black body and its T_B also starts increasing. This can be clearly seen in 85 GHz (H) frequency which shows a jump in T_B values once the melting in snow started.

Figure.5 shows the temporal and spectral variation of T_B at 19, 37 and 85 GHz frequencies of SSM/I at horizontal polarization for Great Himalayan range for year 2007 to 2008. T_B at lower frequency shows higher values in comparison to that of higher frequency. For higher frequency an interesting phenomenon of volume scattering is observed due to which the individual snow grain reduces the T_B by scattering some of radiation out of the sensor field of view. Thus, the value of T_B at higher frequency is low. Also, it shows that T_B is higher in the month of October and decreases from November to March end. However, April onwards the T_B starts increasing because of the onset of melting.

By analyzing T_B with snow cover it was observed that T_B alone is not enough to identify the snow cover hence scattering index (SI) was estimated using equation 1. The variations in snow pack physical properties, such as density, grain size, stratigraphic layering, liquid water content and sub-surface soil state controls scattering signal emitted by snow pack/snow surface. Figure 6 shows the temporal variation of SI for Great Himalayan range for year 2007 to 2008. It is observed that SI values are comparatively higher in between of January to March. These higher values of SI are corresponding to higher amount of snow present in the ground.

Figure.7 shows standing snow up to 82 cm at the observatory location in Great Himalayan range (year 2007 to 2008). Further the graphs in figures 5, 6 and 7 were compared and it was observed that with decrease in T_B the SI increases and significant amount of snow has been observed in the ground corresponding to low T_B and higher SI values.

On the basis of analysis the threshold values of T_B and SI were estimated. From Table 1, it was observed that if in Pir-Panjaj range, T_B lies between 238-251 K at 19 GHz (H), 217-239 K at 37 GHz (H), 198-232 K at 85 GHz (H) and SI lies between 14 to 46 K than snow is present otherwise area is snow free. In Great Himalaya, area is snow covered if T_B lies between 234-245 K at 19 GHz (H), 211- 232 K at 37 GHz (H), 181-227 K at 85 GHz (H) and SI lies between 16 to 57 K. However, for Karakoram range area is snow covered if T_B lies between 205-220 K at 19 GHz (H), 187-211 K at 37 GHz (H), 176-208 K at 85 GHz (H) and SI lies between 6-39 K otherwise the area is snow free.

To develop snow depth algorithms we have used different frequencies shown in Table 2. These frequencies were selected based upon T_B values obtained from satellite data. Snow depth up to 5 cm is corresponding to the T_B (85 GHz (H)) 243-247 K in Pir-Panjaj, 207-233 K in Great Himalaya and between 203-211 K in Karakoram range. However for estimation of snow depth up to 50 cm we have used 37 GHz (H) frequency and this frequency is used for estimation of snow depth if T_B (37 GHz (H)) lies between 234-249 K for Pir-Panjaj, 228-239 K in Great Himalaya and between 212-222 K in Karakoram range. Similarly, for estimation of SD up to 200 cm, 19 GHz (H) and 37 GHz (H) frequencies were used. Here in the analysis we have taken the difference of these frequencies. This T_B difference based algorithms was used if T_B lies between 249-262 K at 19 GHz (H) and 227-234 K at 37 GHz (H) for Pir-Panjaj range, for Great Himalayan range if T_B lies between 243-251 K at 19 GHz (H) and 217-228 K at 37 GHz (H). However for Karakoram range this combination is used when T_B lies between 223-229 K at 19 GHz (H) and 200-212 K at 37 GHz (H).

For snow depth estimation regression analysis was performed between T_B at different frequencies and ground observed snow depth values for different ranges of Himalaya and on the basis of regression analysis the geophysical coefficients were estimated:

For Pir-Panjaj range the estimated coefficients were: $a_1=0.041$, $b_1=-4.111$ at 85 GHz (H), $a_2=-0.017$, $b_2=28.166$ at 37 GHz (H), $a_3=0.069$ and $b_3=78.15$ at 19-37 GHz (H), for Great Himalayan range $a_1= 0.014$, $b_1=0.975$ at 85 GHz (H) , $a_2=-0.197$, $b_2=70.313$ at 37 GHz (H), $a_3=-0.749$, $b_3=84.933$ at 19-37 GHz (H).

However, for Karakoram range $a_1=0.019$, $b_1=-1.2474$ at 85 GHz (H), $a_2=0.1896$, $b_2=-16.846$ at 37 GHz (H), $a_3=-1.498$ and $b_3=95.475$ at 19-37 GHz (H) coefficients were used. Further these algorithms were applied on independent year satellite data and RMSE (root mean square error) between the observed values and algorithms output values was estimated. These different algorithms were found best suited for different range of snow depth values i.e. 85 GHz frequency based algorithm for very less snow depth i.e. 5 cm, 37 GHz frequency based algorithm for 50 cm and 19-37 GHz frequency based algorithm for 200 cm.

Figure 8 shows the comparison between the ground observed snow depth values and satellite data derived snow depth values. These comparisons were done for different Himalayan ranges and a very good correlation was observed for Karakoram range i.e. 0.84 and estimated RMSE is 15 cm. For Great Himalayan range the correlation is 0.77 and RMSE is 16 cm. However, for Pir-Panjal range comparatively less correlation 0.60 is observed and higher RMSE ~ 27 cm, in comparison to other two ranges has been observed. This relatively low performance of the equation in Pir-Panjal is due to moist/wet snow characteristic in Pir-Panjal range. As generally in Karakoram and Great Himalaya the snow is dry and hence microwave based mapping method works better in these ranges.

6. Conclusion

Because of its all weather working capability passive microwave satellite data has the potential to monitor the snow cover of NW-Himalaya on a regular basis. The T_B along with SI can be used to identify the snow cover area.

As the topography of NW-Himalaya is very undulating and the climatic condition at different areas also varies. A single algorithm of snow depth can not be the representative of whole NW-Himalaya. The developed algorithms of snow depth for different Himalayan ranges works satisfactorily. As frequency or wavelength is one of the factor affecting the penetration depth of wave in the snow, thus algorithms for snow depth were formulated using combination of frequencies.

Acknowledgement

The authors are thankful to shri. Ashwagosh Ganju, Director, SASE for his constant motivation and support. The author also extends their sincere thanks to shri. S.K.Dewali, shri. S.P.Reddy, Shri. Himanshu for providing technical supports during preparation of the manuscript. The authors would also like to acknowledge all the SASE persons who have collected

the ground data. Thanks are also due to Sahil Sood, Senior Research Fellow, SASE for dedicated help and scientific discussion. The SSM/I data were made available by the National Snow and Ice data center, University of Colorado, Boulder.

References

- [1] Hollinger. J., "DMSP SSM/I calibration/validation, Final report, part 1 and 2, Nav.Res.Lab", Washington, D.C., 1991.
- [2] Khan.V.M. and Holko L., "Snow cover characteristic in Areal Sea Basin from different data source and their relation with river runoff," *Journal of Marine system*. Vol.76 (3), pp-254-262, 2009.
- [3] Schoner.W., Auer. I. and Bohm R., "Long term trend of snow depth at sonnblick (Austrian Alps) and its relation to climate change," *Hydrological progress*, Vol.23 (7), pp-1052-1063, 2009.
- [4] Foster. J.L., Hall. D.K. and Chang A.T.C., "An overview of passive microwave sensor and Result" *Reviews of geophysics and space physics*. Vol.22, pp-195-208, 1984.
- [5] Grody.N.C. and Basist.A.N., "Global identification of snow cover using SSMI/ measurements," *IEEE Transaction on Geosciences and Remote Sensing*, vol 34, pp237-252, 1996.
- [6] Singh K.K., Mishra V.D. and Negi H.S. "Evaluation of Snow Parameters Using Passive Microwave Remote Sensing" *Defence Science Journal*, V57, No 2, 2007.
- [7] Negi.H.S., Thakur.N.K. and Mishra.V.D, "Estimation and Validation of snow surface temperature using MODIS data for snow-avalanche studies in NW Himalaya" *Journal of the Indian Societies of Remote sensing*. Vol.35, pp-288, 2007
- [8] Sharma. S.S and Ganju. A., "Complexities of avalanche forecasting in western Himalaya-an overview" *Cold region science and technology*. Vol.31, pp-95-102., 2000.

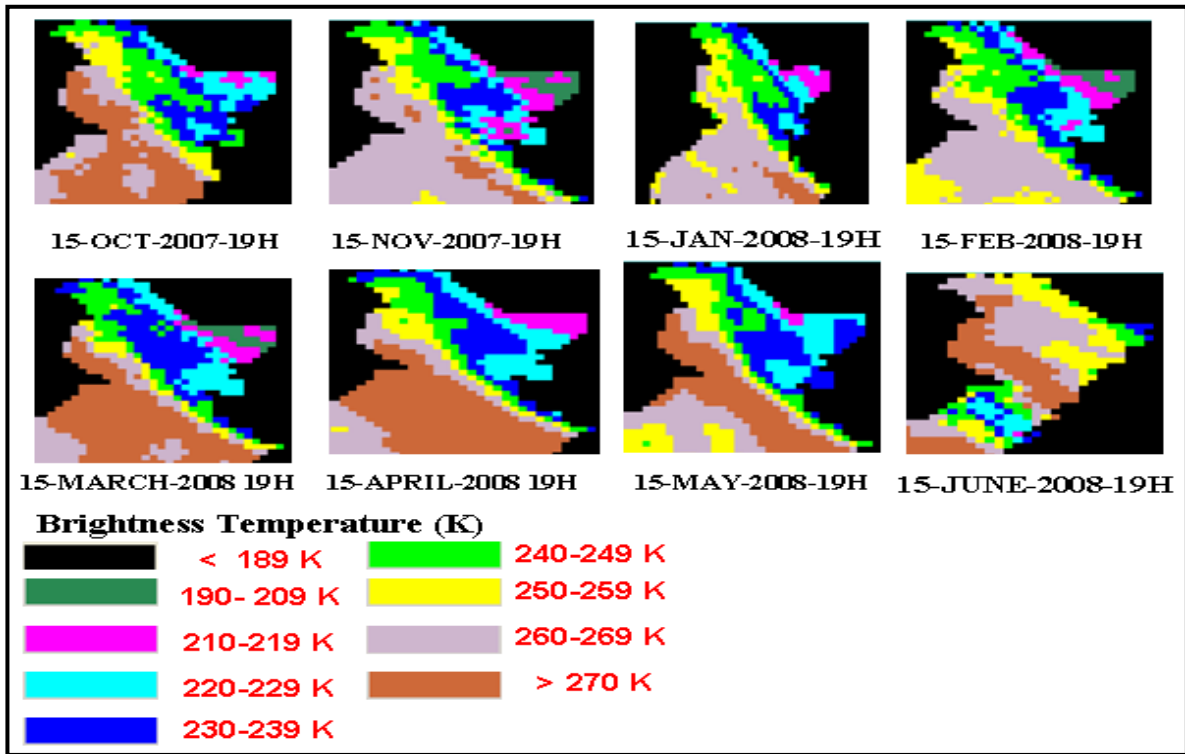


Figure 3: Temporal and spatial variation of T_B at 19 GHz (H) for NW Himalaya (year: 2007 to 2008)

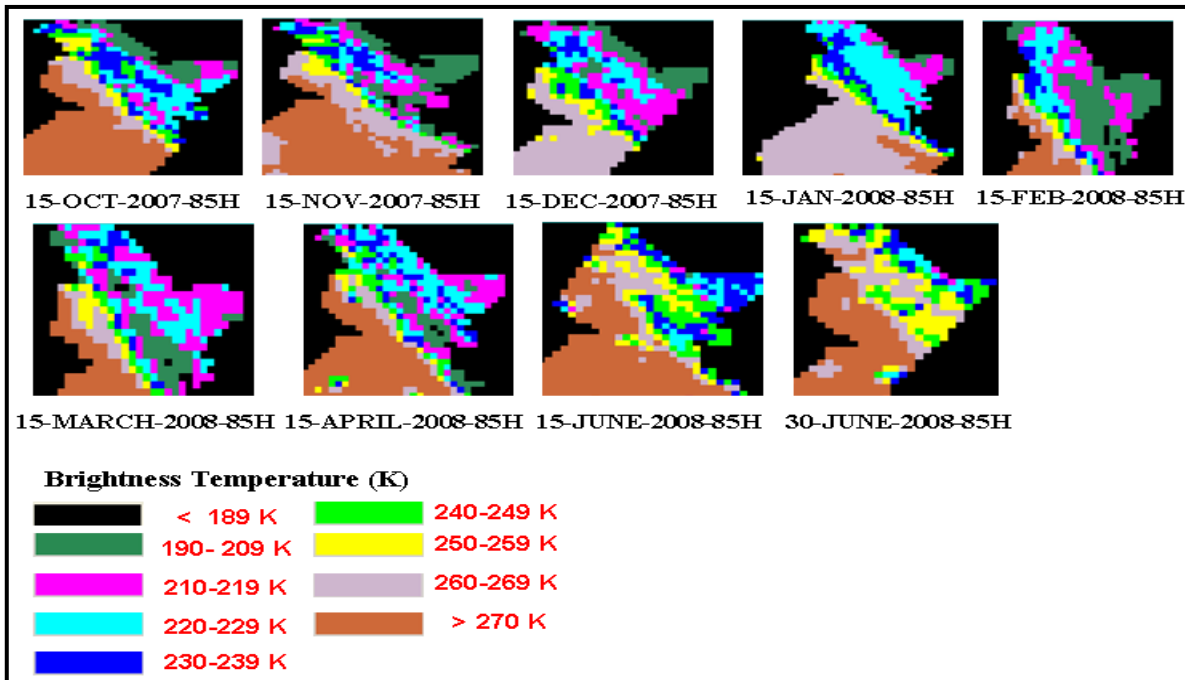


Figure 4: Temporal and spatial variation of T_B at 85 GHz (H) for NW Himalaya (year: 2007 to 2008)

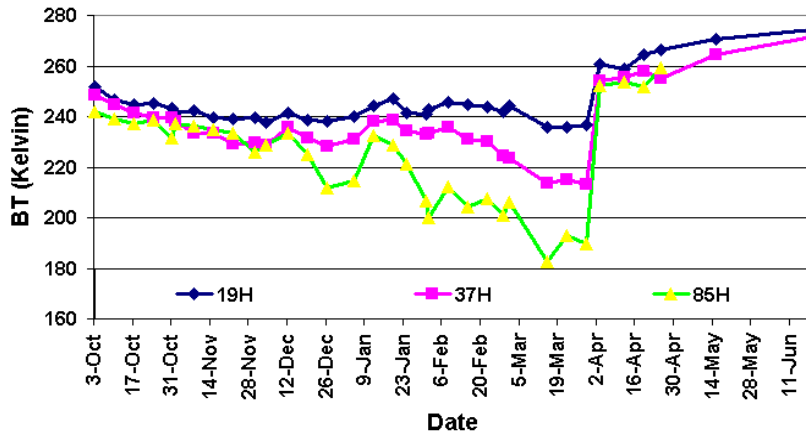


Figure 5: Temporal and spectral variation of T_B at 19, 37 and 85 GHz (H) for Great Himalaya (year: 2007 to 2008)

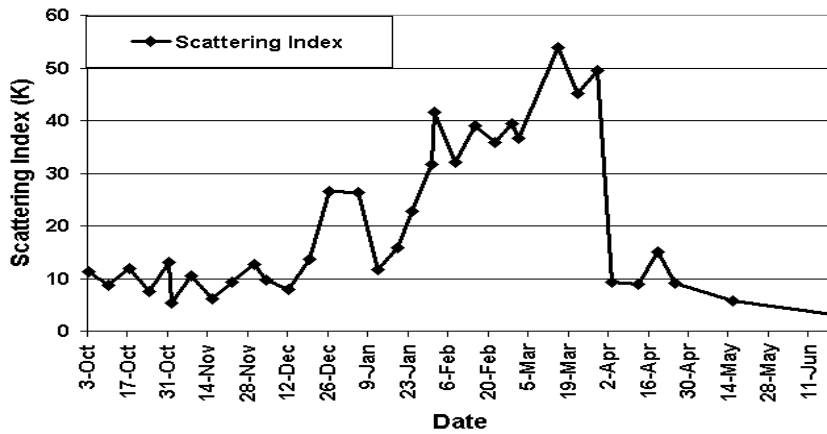


Figure 6: Temporal variation of scattering index (SI) for Great Himalaya (year: 2007 to 2008).

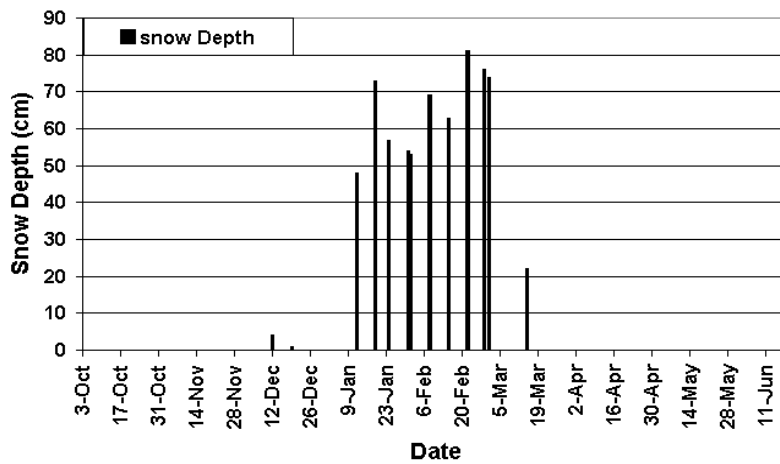


Figure 7: Temporal variation of manually observed snow depth values for Great Himalaya (year: 2007 to 2008).

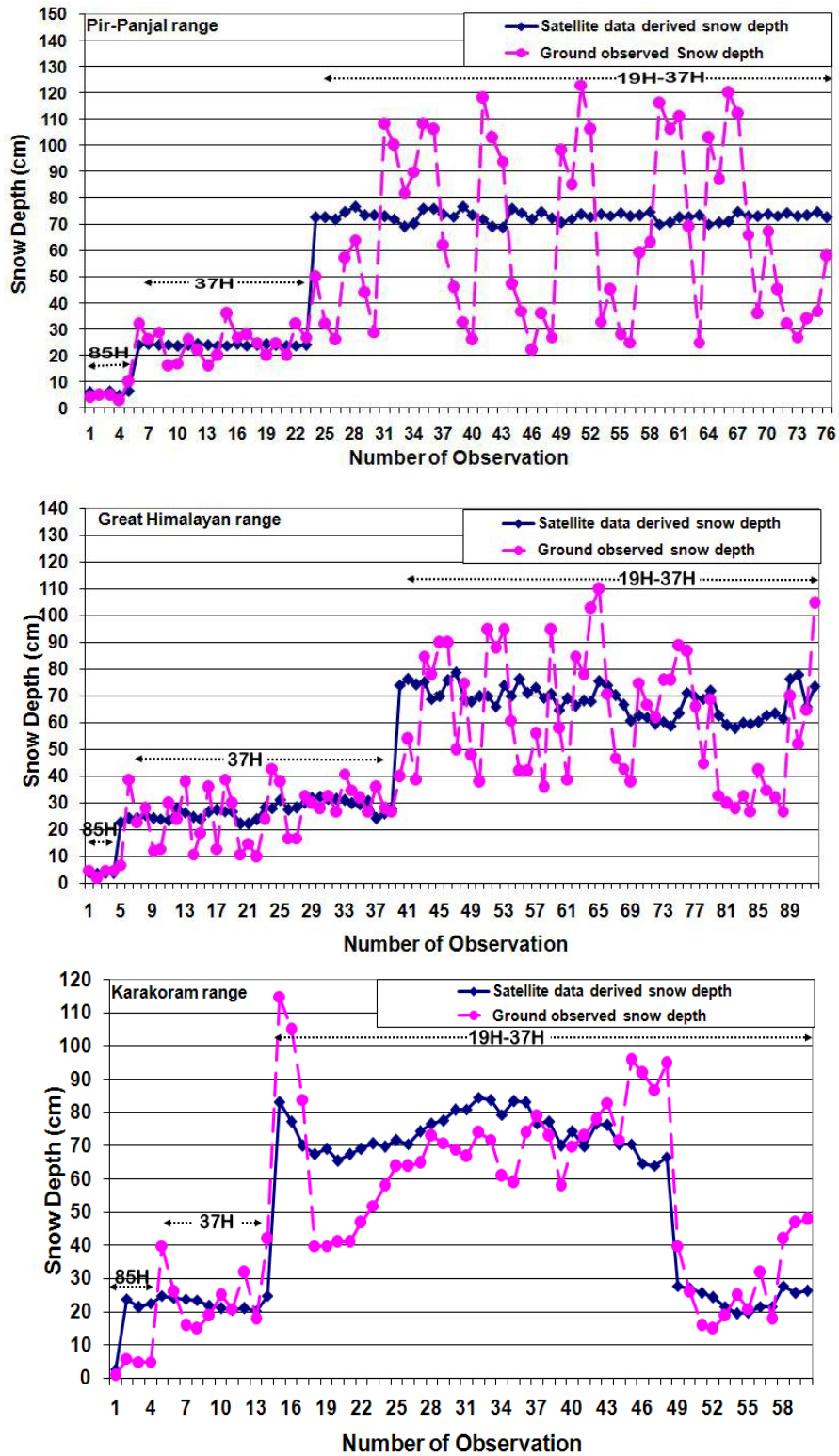


Figure 8. Validation of satellite data derived and ground observed snow depth for year 2000.

Table 1: Threshold value of T_B and SI for snow cover of different ranges of NW Himalaya.

NW Himalayan ranges	Year	19GHz		37 GHz		85 GHz		Scattering Index (K)	
		Max T_B (K)	Min T_B (K)	Max T_B (K)	Min T_B (K)	Max T_B (K)	Min T_B (K)	Max	Min
Pir-Panjal range	2007-2008	253	240	243	224	241	205	36	8
	2008-2009	251	239	239	209	235	204	41	12
	2009-2010	245	237	235	218	225	189	50	18
	2010-2011	253	237	239	216	227	193	58	18
	Average	251	238	239	217	232	198	46	14
	Great Himalayan range	2007-2008	247	236	236	213	233	182	54
2008-2009		247	237	235	213	223	189	52	21
2009-2010		245	233	231	202	230	170	66	16
2010-2011		242	230	230	213	222	180	58	19
Average		245	234	232	211	227	181	57	16
Karakoram range	2008-2009	220	203	206	185	208	174	43	8
	2009-2010	217	205	212	190	206	180	34	2
	2010-2011	225	208	214	185	210	172	41	10
	Average	220	205	211	187	208	176	39	6

Table 2. Selection criteria for different snow depth algorithms.

Snow Depth (cm)	Channel (GHz)	Pir-Panjal range (T_B in K)	Great Himalaya (T_B in K)	Karakoram range (T_B in K)
5	85H	243-247 K	207-233 K	203-211 K
50	37H	234-249 K	228 -239-K	212-222 K
200	19H	249-262 K	243 -251 K	223-229 K
	37H	227-234 K	217-228 K	200-212 K